Supporting Information for "Rupture evolution of the 2006 Java tsunami earthquake and the possible role of splay faults"

Wenyuan Fan[a,b], Dan Bassett[a,c], Junle Jiang[a], Peter M. Shearer[a], Chen Ji[d,e]

[a] *Scripps Institution of Oceanography, UC San Diego, La Jolla, CA 92093-0225, USA.*
[b] *Woods Hole Oceanographic Insitution, Woods Hole, MA 02543, USA.*
[c] *GNS Science, Lower Hutt, 5010, New Zealand.*
[d] *Earth Research Institute, UC, Santa Barbara, Santa Barbara, CA 93106, USA.*
[e] *Department of Earth Science, UC, Santa Barbara, Santa Barbara, CA 93106, USA.*

Contents of this file

Preprint submitted to Tectonophysics *September 28, 2017*

Text S1: Back-projection uncertainty analysis:

Following *Fan and Shearer* (2016), we perform jackknife resampling over the records used for back-projection *Efron and Tibshirani* (1994). For the ith resampling, we suppose we have n stations to estimate peak energy location (latitude and longitude) of each 20 s seismic radiation:

$$\hat{Lat} = BP^{lat}(n) \quad \hat{Lon} = BP^{lon}(n) \tag{1}$$

where $\hat{Lat}$ and $\hat{Lon}$ are location estimations. When the ith station is excluded, the estimations can be written as $\hat{Lat}_i = BP_i^{lat}(i)$ and $\hat{Lon}_i = BP_i^{lon}(i)$. Then the jackknife estimate of standard errors (SE) are

$$\hat{SE}_{Lat} = \left(\frac{n-1}{n} \sum_{i=1}^{n} (\hat{Lat}_i - \bar{Lat}) \right)^{1/2} \tag{2}$$

$$\hat{SE}_{Lon} = \left(\frac{n-1}{n} \sum_{i=1}^{n} (\hat{Lon}_i - \bar{Lon}) \right)^{1/2} \tag{3}$$

where $\bar{Lat}$ and $\bar{Lon}$ are the averages locations.

References

Bassett, D., and A. B. Watts (2015a), Gravity anomalies, crustal structure, and seismicity at subduction zones: 1. Seafloor roughness and subducting relief, *Geochem. Geophys. Geosyst.*, *16*(5), 1508–1540, doi: 10.1002/2014GC005684.

Bassett, D., and A. B. Watts (2015b), Gravity anomalies, crustal structure, and seismicity at subduction zones: 2. Interrelationships between fore-arc structure and seismogenic behavior, *Geochem. Geophys. Geosyst.*, *16*(5), 1541–1576, doi:10.1002/2014GC005685.

Efron, B., and R. J. Tibshirani (1994), *An introduction to the bootstrap*, CRC Press.

Fan, W., and P. M. Shearer (2016), Local near instantaneously dynamically triggered aftershocks of large earthquakes, *Science*, *353*(6304), 1133–1136, doi:10.1126/science.aag0013.

International Seismological Centre (2013), *On-line Bulletin*, Int. Seis. Cent., Thatcham, United Kingdom (2013).

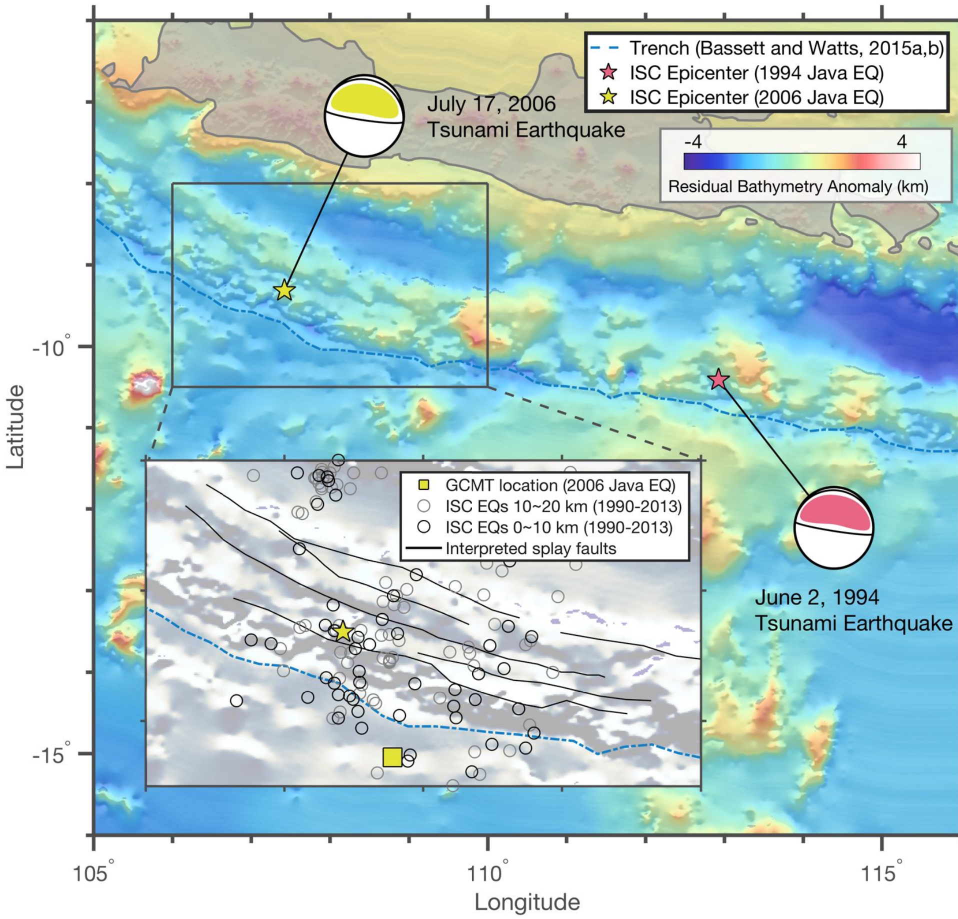

Figure S1: Residual bathymetry anomaly, splay faults at Java subduction zone and shallow seismicity near the 2006 Java tsunami earhtquake. Insert: black circles are earthquakes (EQ) from 1993-2013 ISC catalog with M > 4 and depth shallower than 10 km, gray circles are earthquakes (EQ) from 1993-2013 ISC catalog with M > 4 and depth in between of 10 and 20 km (*International Seismological Centre*, 2013). Black lines are the interpreted fault traces. Trench-axis is from *Bassett and Watts* (2015a,b).

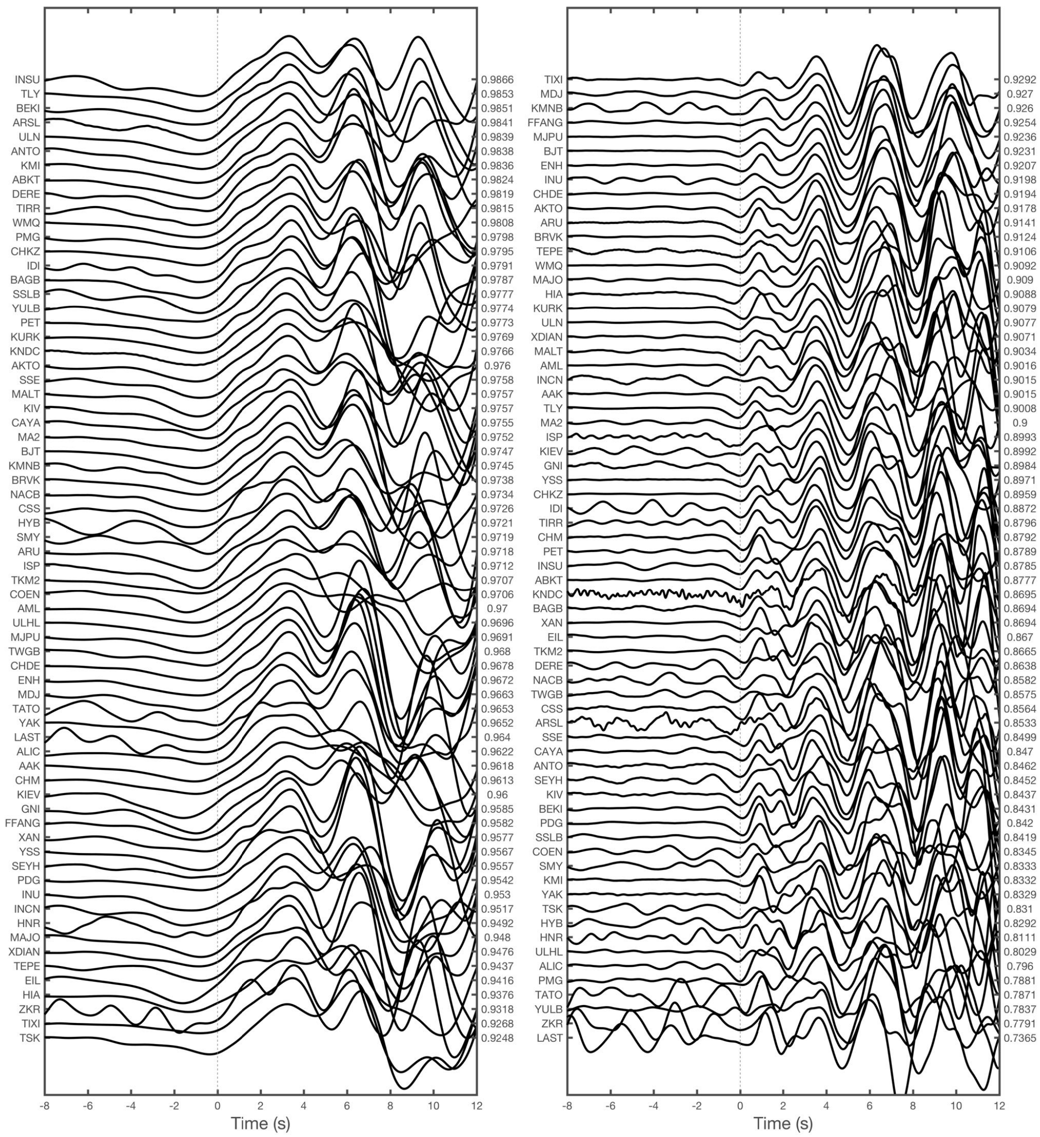

Figure S2: P-wave velocity seismogram alignments. 0.05–0.3 Hz (LF, Left panel) and 0.3–1 Hz (HF, right panel). The onset of the P wave begins at 0s. The records (station name left axis) are sorted by average cross-correlation coefficients (right axis).

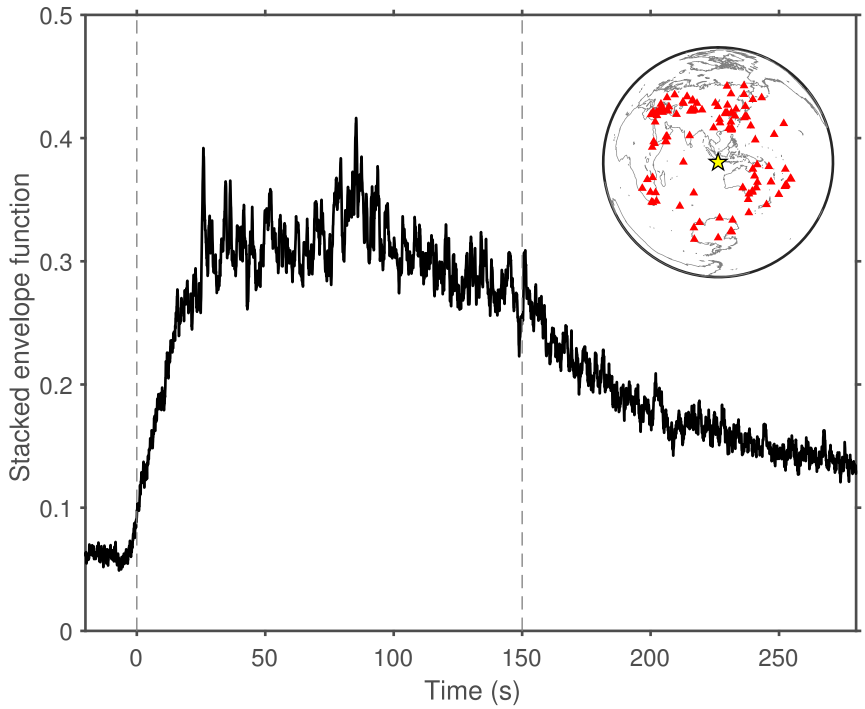

Figure S3: Stacked envelope function. Stations used for the calculation are shown in the insert. The P-wave seismograms are filtered at 1–5 Hz. The envelope functions are calculated with a standard Hilbert transform without smoothing. Each envelope function is self-normalized before stacking. The stacked envelope function is divided by the number of stations.

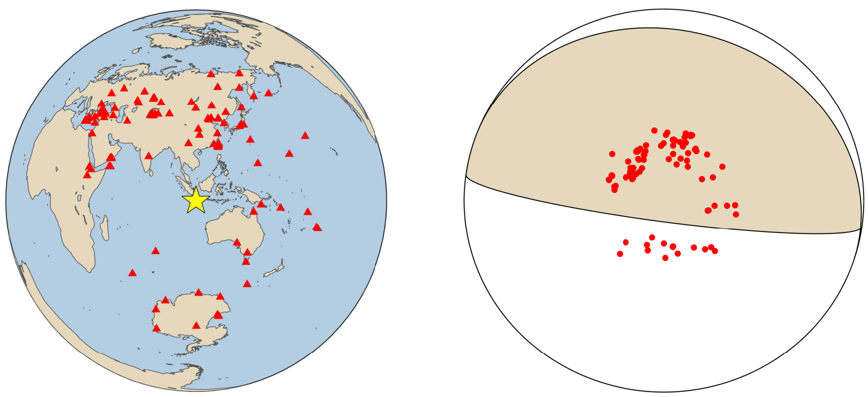

Figure S4: Globally distributed stations and their P-wave polarities with respect to the GCMT solution of the mainshock.

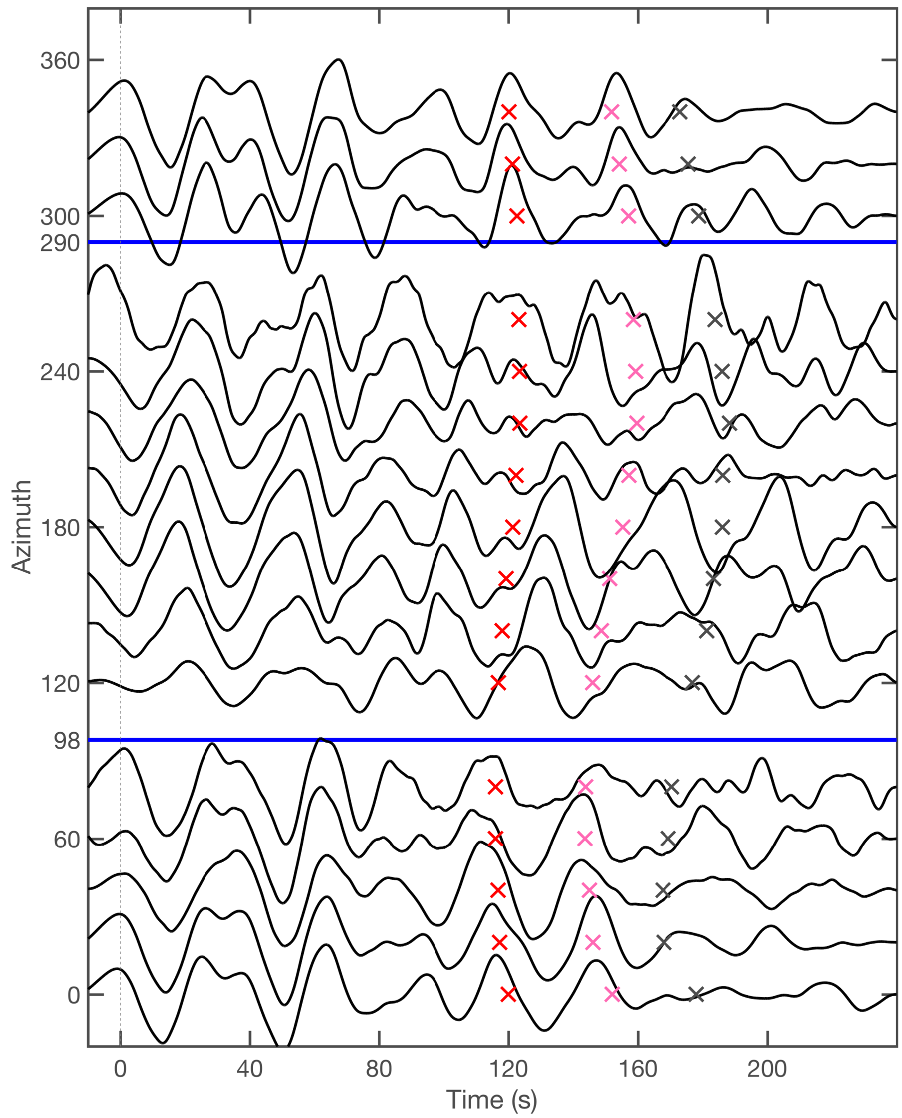

Figure S5: Aligned velocity seismograms (0.02-0.05 Hz) from globally distributed stations (Figure S4). Blue lines shows the nodal plane strikes of GCMT. Predicted travel time shows as crosses with color corresponding to Figure 3.